Available online at www.sciencedirect.com
SCIENCE DIRECT®
Journal of Sound and Vibration 280 (2005) 657–680
JOURNAL OF SOUND AND VIBRATION
www.elsevier.com/locate/jsvi

Control of uncertain non-linear systems via adaptive backstepping

V. Mañosa[a,*], F. Ikhouane[b], J. Rodellar[b]

[a] *Departament de Matemàtica Aplicada III, Universitat Politècnica de Catalunya, Colom 1, Terrassa, 08222 Barcelona, Spain*
[b] *Jordi Girona 1-3, 08034 Barcelona, Spain*

Received 3 July 2003; accepted 12 December 2003

Abstract

Models of physical non-linear systems are prone to different kinds of uncertainties. This paper presents a backstepping-based adaptive control designed for a class of one degree-of-freedom uncertain non-linear systems. The true system does not need to be known for the control design. A functional description is assumed with uncertain coefficients and an uncertain residual function. These uncertainties are bounded and lump the discrepancies between the adopted description and the real behaviour. The adaptive controller is able to handle these uncertainties and make the closed loop globally uniformly ultimately bounded when the system is subject to an unknown excitation from which a bound is known. One goal is that the transient and asymptotic performances depend explicitly on the design parameters. This feature of the control scheme establishes the main difference with other control methods used to control non-linear systems, in particular chaotic systems. The efficiency of the approach is tested by numerical simulations on Duffing oscillators and systems with non-linear and hysteretic stiffness under external loads.

1. Introduction

Models of real physical systems usually contain different types of uncertainties. These uncertainties are typically due to unmodelled dynamics, unknown external disturbances, bad knowledge of the values of the parameters and others. Therefore the design of robust control schemes, able to handle a large class of uncertain systems, is needed.

*Corresponding author. Tel.: +34-93-739-8257; fax: +34-93-739-8225.
E-mail addresses: victor.manosa@upc.es (V. Mañosa), faycal.ikhouane@upc.es (F. Ikhouane), jose.rodellar@upc.es (J. Rodellar).

0022-460X/$ - see front matter © 2004 Elsevier Ltd. All rights reserved.
doi:10.1016/j.jsv.2003.12.033

In this paper a backstepping-based adaptive control scheme is presented in order to drive the response of a class of uncertain non-linear second order one-dimensional systems to a desired state when subjected to an external excitation. Backstepping refers to a recent approach for design of stabilizing controllers for non-linear systems (see Ref. [1]). As noted in Ref. [2], adaptive control systems and, in particular, adaptive backstepping controllers seem to be good candidates for controlling uncertain non-linear systems.

In this paper, a switching σ-modification [3,4] and a new term that incorporates part of the information on the uncertainty is used with the objective of driving the output to a neighbourhood of a reference trajectory, thus reducing the vibrations induced by the external excitations. The resulting closed loop is globally uniformly ultimately bounded [5] and the output can be made asymptotically arbitrarily small by choosing appropriate design parameters, since the analysis presented in the paper evidences that both the transient and the asymptotic performance depend explicitly on specific design parameters.

The paper is structured as follows. In Section 2, the control scheme design and implementation are presented, together with the main results of the paper, which ensure the globally uniform boundedness of the closed-loop responses and analyze the transient and asymptotic behaviour. Since the proofs of these results follow standard arguments, they are presented (for the sake of completeness) in Appendix A.

In Section 3, the control scheme is applied to a Duffing oscillator which (in open loop) displays a chaotic motion regime. Since the seminal paper [6] (see also Ref. [7]), a significant research effort has been done in two directions: (1) to introduce chaotic behaviours in systems with regular dynamics for targeting purposes as first steps in a control scheme [8], and (2) to drive chaotic trajectories to a desired state. Duffing's system (introduced in 1918) is a simple model to explain the motions of several systems, like a magnetoelastic beam under forced vibrations in the non-uniform field of two permanent magnets [9–11], and constitutes a paradigmatic example of an oscillator leading to "chaotic" motions caused by an external forcing. Duffing's oscillator also appears to be of interest in structural dynamics, as in modelling and identification of base isolation devices [12] and hydraulic dampers [13].

Backstepping design has recently been used for synchronization and robust control of chaotic systems (in particular, Duffing's oscillator), see Refs. [2,14]. The control scheme in this paper allows the designer to tune the design coefficients in an explicit way to obtain the closed-loop desired behaviour both for the transient and the asymptotic tracking. This gives a difference to the mentioned works. In fact, other control methods used to control chaos as the Ott–Grebogi–Yorke (OGY) method (see Refs. [6,7]) can exhibit a very bad transient performance since the control must wait until the system is close enough to certain region. This is, in general, not the case of the control presented here, which acts globally and gives the possibility of tuning the transient performance. This is one of the main goals of this paper, and encourages the authors to agree with the conclusions in Ref. [2] and to propose adaptive backstepping schemes as a good option to control uncertain non-linear systems.

In structural systems, feedback controllers in the presence of non-linear components have been primarily encountered when dealing with smart actuators and base isolation schemes. In Section 4, the efficiency of the backstepping control scheme is tested when dealing with the suppression of the vibrations in non-linear uncertain isolation devices induced by seismic excitations.

Duffing-like oscillators have been chosen to describe the restoring force appearing in structural systems [12,13]. However, it has been noted that some real systems do not fit the mathematical model given by the Duffing oscillator, see Refs. [13,15]. In Ref. [16] an identification procedure using Chebyshev Polynomials reveals that the mathematical representation of the behaviour of some real physical systems must include terms beyond the cubic. In Section 4.2, the control scheme is applied to a model of a base isolation system with a non-linear stiffness given by a high order polynomial. In Section 4.3, the control is applied to a base isolation scheme with a hysteretic restoring force described by the Bouc-Wen model [17]. This model lies within the class of differential hysteretic models and has been widely used in structural dynamics, particularly to describe rubber bearing base isolation schemes [18].

2. Problem statement and main results

2.1. Problem statement

In this section an adaptive control scheme is developed for systems of the form

$$\begin{aligned} \dot{x}_1 &= x_2, \\ \dot{x}_2 &= \alpha x_2 + Q(x_1, t) + e(t) + f_c(t), \end{aligned} \tag{1}$$

where $x_1 \in \mathbb{R}$ and $x_2 \in \mathbb{R}$ are the state variables, $e(t) \in \mathbb{R}$ is an external disturbance, $f_c(t) \in \mathbb{R}$ is the control input and

$$Q(x, t) = \sum_{k=1}^{n} \delta_k \psi_k(x, t) + R(x, t), \tag{2}$$

where the coefficients δ_k are real uncertain parameters, $\psi_k(x, t)$ are known locally Lipschitz functions and $R(x, t)$ is an unknown residual term. The following assumptions complete the description of system (1).

Assumption 1. The coefficient α is an unknown parameter which lies within an interval $[-\alpha_m, \alpha_m]$, where α_m is known.

Assumption 2. The constant vector $\mathbf{\Theta}_\delta = (\delta_1, \delta_2, \ldots, \delta_n)^{\mathrm{T}}$ is unknown but lies within a known sphere. That is $\|\mathbf{\Theta}_\delta\| \leqslant M_\delta$ for a known positive constant M_δ.

Assumption 3. The function $R(x, t)$ is unknown but is assumed to be locally Lipschitz and such that $|R(x, t)| \leqslant \bar{R}$, for all $x \in \mathbb{R}$ and $t \geqslant 0$, where $\bar{R}$ is a known positive constant.

Assumption 4. The exciting signal $e(t)$ is unknown but bounded in the form $|e(t)| \leqslant E$ for all $t \geqslant 0$, where E is a known positive constant.

As shown in further sections, different systems can be represented within the form considered above.

The objective of this paper is to design a backstepping-based adaptive control law for systems (1)–(2) (under Assumptions 1–4) satisfying the following specifications:

1. The closed loop is globally uniformly ultimately bounded.
2. Let $y_r(t)$ be a given known bounded reference signal (where $\dot{y}_r$ and $\ddot{y}_r$ are known, bounded and piecewise continuous). The tracking error $x_1(t) - y_r(t)$ can be reduced both in the transient and asymptotically by an explicit choice of the design parameters.

2.2. Control design

System (1) can be rewritten in the form

$$\begin{aligned} \dot{x}_1 &= x_2, \\ \dot{x}_2 &= \mathbf{\Phi}(x_1, x_2, t)^{\mathrm{T}}\mathbf{\Theta} + R(x_1, t) + e(t) + u(t), \end{aligned} \tag{3}$$

where $\mathbf{\Phi}(x_1, x_2, t)^{\mathrm{T}} = (x_2, \psi_1(x_1, t), \ldots, \psi_n(x_1, t))$ and $\mathbf{\Theta}^{\mathrm{T}} = (\alpha, \delta_1, \ldots, \delta_n)$.

From Assumptions 1 and 2, it follows that

$$\|\mathbf{\Theta}\| \leqslant \sqrt{\alpha_m^2 + M_\delta^2} \triangleq M. \tag{4}$$

Now introduce the following auxiliary variables:

$$\begin{aligned} z_1 &= x_1 - y_r \quad \text{(tracking error)}, \\ z_2 &= x_2 - \alpha_1, \\ \alpha_1 &= -c_1 z_1 + \dot{y}_r \quad \text{(stabilizing function)}. \end{aligned} \tag{5}$$

An adaptive control scheme is proposed below. It is obtained using adaptive backstepping design. The main ingredient of the backstepping design is the co-ordinate change (5). As usual in Lyapunov-based methods, the design combines the choice of a Lyapunov function (for the system in the new co-ordinates) with the design of the control law as well as the parameter update law (see Ref. [1, Chapters 3 and 4]). In this sense, both the control law (6) and the parameter estimate law (7) below have been obtained when trying to minimize the derivative of the Lyapunov function (A.1) given in Appendix A. A switching σ-modification has been added to the parameter update law, as in Ref. [3], to prevent parameter drift.

Adaptive control law:

$$u(t) = -\mathbf{\Phi}(x_1, x_2, t)^{\mathrm{T}}\hat{\mathbf{\Theta}} - z_1 - c_2 z_2 - c_1 x_2 - \mathrm{sg}(z_2)\mathrm{cf}(|r z_2|)r + c_1\dot{y}_r + \ddot{y}_r. \tag{6}$$

Parameter estimate law:

$$\begin{aligned} \dot{\hat{\mathbf{\Theta}}} &= \mathbf{\Gamma}\mathbf{\Phi}(x_1, x_2, t)z_2 - \mathbf{\Gamma}\sigma_{\mathbf{\Theta}}(\|\hat{\mathbf{\Theta}}\|)\hat{\mathbf{\Theta}}, \\ \hat{\mathbf{\Theta}}(0) &= \hat{\mathbf{\Theta}}_0. \end{aligned} \tag{7}$$

In the above expressions, c_1 and c_2 are positive design parameters and $r = \bar{R} + E$ is a bound on the uncertainty in model (1). It is obtained by adding the bound on the residual term $R(x_1, t)$ and the bound on the excitation signal $e(t)$ (see Assumptions 3 and 4). $\mathbf{\Gamma}$ is a positive definite design

matrix and $\mathrm{cf}(y) = \sigma(y/\varepsilon_1)$, $\sigma_\Theta(y) = \bar{\sigma}\sigma(y/M)$, where

$$\sigma(y) = \begin{cases} 0, & y < 1, \\ y - 1, & y \in [1, 2], \\ 1, & y > 2, \end{cases}$$

$$\mathrm{sg}(y) = \begin{cases} -1, & y < -\dfrac{1}{1+r}\varepsilon_2, \\ \dfrac{1+r}{\varepsilon_2} y, & y \in \left[-\dfrac{1}{1+r}\varepsilon_2, \dfrac{1}{1+r}\varepsilon_2\right], \\ 1, & y > \dfrac{1}{1+r}\varepsilon_2, \end{cases}$$

where ε_1, ε_2 and $\bar{\sigma}_\Theta$ are positive design parameters.

Remark. In general, in order to rewrite systems in form (1) into form (3), proceed as follows: All the terms having a known functional description and parametric uncertainties are included in the term $\mathbf{\Phi}(x_1, x_2, t)^{\mathrm{T}}\mathbf{\Theta}$. All the bounded uncertain terms depending on x_1 and t not having a functional description must be added in the term $R(x_1, t)$. The control variable u includes the real active control f_c plus all the terms of the model with a known functional description and without parametric uncertainties. That is, the control u contains all the terms of the model that are computable (see, for instance, Ref. [19]). This trick helps avoid unnecessary terms in the dynamic estimator $\hat{\mathbf{\Theta}}$, given by Eq. (7).

2.3. Main results

The following results assure that system (3) can be stabilized using the control scheme presented above, and that its performance can be improved by an accurate selection of the design parameters.

Theorem 1. *The orbits of the closed loop composed of system* (3), *under Assumptions* 1–4, *and the controller defined in Eqs.* (6) *and* (7) *are globally uniformly ultimately bounded. Moreover the control signal is bounded.*

Theorem 2. *Consider system* (3) *subject to Assumptions* 1–4 *along with the control law given by Eqs.* (6) *and* (7). *Then the following statements hold*:

(a) *The asymptotic tracking error is given by*

$$\|z_1\|^2_{r.m.s.,[t_0,\infty]} \triangleq \lim_{T\to\infty} \frac{1}{T}\int_{t_0}^{t_0+T} z_1^2(t)\,\mathrm{d}t \leqslant \frac{4\varepsilon_1 + 2\varepsilon_2}{c_1}, \tag{8}$$

for any $t_0 \geqslant 0$.

(b) *The transient tracking error is given by*

$$\|z_1\|^2_{r.m.s.,[0,T]} \triangleq \frac{1}{T}\int_0^T z_1^2(t)\,\mathrm{d}t \leqslant \frac{\max(1, \lambda_{max}(\mathbf{\Gamma}^{-1}))}{\min(c_1, c_2, \frac{3}{4}\bar{\sigma})} \frac{(\frac{39}{4}\bar{\sigma}M^2 + 4\varepsilon_1 + 2\varepsilon_2)}{2c_1 T} + \frac{4\varepsilon_1 + 2\varepsilon_2}{c_1}, \tag{9}$$

for all $T \geqslant 0$, *where* λ_{max} *denotes the maximum eigenvalue.*

From Theorem 2 the following conclusions are drawn about the role of the parameters in the control law:

(i) The tracking performances (both transient and asymptotic) are expressed explicitly as a functions of design parameters.
(ii) To reduce the tracking performance (transient and asymptotic) either increase the gains c_1, c_2, and $\bar{\sigma}$ or decrease ε_1, ε_2. However, since they enter directly into the control law, this means that improving the closed-loop behaviour may be done at the expense of an increase in the control signal amplitude. That is, a trade-off between good performance and reasonable control amplitude should be made.
(iii) The transient tracking error can be reduced by increasing the eigenvalues of the adaptation gain $\mathbf{\Gamma}$ as long as $\lambda_{max}(\mathbf{\Gamma}^{-1}) > 1$. This increase has no effect on the asymptotic tracking performance.
(iv) The transient performance depends on the accuracy of the estimate of the bounds of the uncertain parameters through M.

The proofs of these theorems are presented in Appendix A.

In order to test the proposed control scheme it has been applied, by means of numerical simulations, in three different cases presented in Sections 3 and 4. In these examples, the ratio of the root mean square norm of the control signal $u(t)$ versus the root mean square norm of the external excitation $e(t)$ (in an appropriate time interval $[0, T]$), is proposed to give a relative measure of the *strength* of the control action, that is

$$S_{r.m.s.,[0,T]} \triangleq \frac{||u||_{r.m.s.,[0,T]}}{||e||_{r.m.s.,[0,T]}}, \tag{10}$$

where, as usual, the root mean square norm is computed as

$$||y||_{r.m.s.,[0,T]} \triangleq \sqrt{\frac{1}{T}\int_0^{\mathrm{T}} y^2(t)\,\mathrm{d}t}.$$

The following index is proposed to give a relative measure of the *performance*:

$$P_{r.m.s.,[0,T]} \triangleq \frac{||z_1^{con}||_{r.m.s.,[0,T]}}{||z_1^{unc}||_{r.m.s.,[0,T]}}, \tag{11}$$

where $z_1(t)^{con} = x_1^{con}(t) - y_r(t)$ is regulation/tracking error variable in closed loop, and $z_1(t)^{unc} = x_1^{unc}(t) - y_r(t)$ is regulation/tracking error variable in open loop.

3. Application: control of a Duffing oscillator

3.1. System description and control design

Duffing's oscillator is the well-known second order differential equation with a cubic non-linear stiffness given by Ref. [9]

$$\ddot{x} + \delta\dot{x} - \beta x + x^3 = e(t) + f_c(t). \tag{12}$$

After the works of Moon and Holmes [9–11], this system appears to be a simple model for the motion of a magnetoelastic beam under forced vibrations in the non-uniform field of two permanent magnets. In Eq. (12), x represents the displacement of the beam and f is the resulting external force. Now consider that the external force includes an exciting force (disturbance) $e(t)$ plus an active control force $f_c(t)$. Introducing the state space variables $(x_1, x_2) = (x, \dot{x})$, the Duffing's equation (12) can be written in the following form:

$$\begin{aligned} \dot{x}_1 &= x_2, \\ \dot{x}_2 &= \mathbf{\Phi}(x_1, x_2, t)^{\mathrm{T}}\mathbf{\Theta} + e(t) + f_c(t) - x_1^3, \end{aligned} \tag{13}$$

where $\mathbf{\Phi}(x_1, x_2, t) = (x_2, x_1)$, $\mathbf{\Theta}^{\mathrm{T}} = (-\delta, \beta)$. If (following the indications given in Section 2.2) we sets $u(t) \coloneqq f_c(t) - x_1^3(t)$, system (13) fits in the class of systems (3), with $R(x_1, t) \equiv 0$. The "control variable" is now $u(t)$ and is obtained with the adaptive feedback control scheme (6)–(7), but observe that the final active control force acting on the system is then $f_c(t) = u(t) + x_1^3(t)$, yielding to

$$f_c(t) = \hat{\delta}x_2 - \hat{\beta}x_1 + x_1^3 - z_1 - c_2 z_2 - c_1 x_2 - \mathrm{sg}(z_2)\mathrm{cf}(|rz_2|)r + c_1\dot{y}_r + \ddot{y}_r.$$

3.2. Simulation results

In this section the efficiency of the control scheme presented in Section 2.2 will be tested. The real parameters of system (12), which are unknown for the controller, are given by $\beta = 1$, $\delta = 0.25$, and the external excitation (also unknown for the controller) is given by $e(t) = \gamma\cos(\omega t)$ with $\gamma = 0.3$ and $\omega = 1$. With these values of the parameters, system (12) apparently exhibits chaotic motions and a strange attractor [9, pp. 82–91].

For the control implementation, it is assumed that $|e(t)| \leqslant E \triangleq 0.45$ (observe that $r = E$, since $R = 0$) and $M = 1.5\|\mathbf{\Theta}_{\delta}^{(nom)}\| = 1.5\|(\beta, \delta)\| = 1.5462$, which is a 50% of uncertainty added to $\max_{t\in[0,\infty)}|e(t)|$ and $\|\mathbf{\Theta}_{\delta}^{(nom)}\|$, respectively.

The design parameters are set to be: $\mathbf{\Gamma} = 10\mathbf{I}_2$, $\varepsilon_1 = 1$, $\varepsilon_2 = 2$, $c_1 = 0.75$, $c_2 = 5$ and $\bar{\sigma} = 0.25$, where $\mathbf{I}_2$ is the 2×2 identity matrix. The initial conditions for the parameter estimation are chosen $\hat{\beta}(0) = 0$ and $\hat{\delta}(0) = 0$.

Figs. 1 and 2 show the performance of both the open- and closed-loop responses (dashed and solid lines, respectively) when reference tracking signals $y_r(t) \equiv 0$ and $y_r(t) \equiv 1$ are fixed, respectively. It can be observed that the controlled orbits tend to a periodic motion, contained in a ball of ultimate boundedness, whose radius can be reduced increasing the gains c_1, c_2 and $\bar{\sigma}$. In the case $y_r(t) \equiv 0$, the performance index (11) for 70 s is $P_{r.m.s.,[0,70]} = 0.0518$, resulting in a reduction in the regulation error for x_1 of 94.82%. When $y_r(t) \equiv 1$, $P_{r.m.s.,[0,70]} = 0.0974$, hence the regulation error has been reduced in a 90.26%.

Observe that the transient response is very fast in reaching this neighbourhood, but this is at the cost of a high control action in comparison with the external excitation. Indeed, for the case where $y_r(t) \equiv 0$, the strength index (10) is $S_{r.m.s.,[0,70]} = 1.6341$. In the case where $y_r(t) \equiv 1$, $S_{r.m.s.,[0,70]} = 1.1306$.

In Fig. 3 the open- and closed-loop responses are shown when a reference tracking signal $y_r(t) = 1 + 0.5\cos(t)$ is considered. Fig. 4 displays both the history of the reference

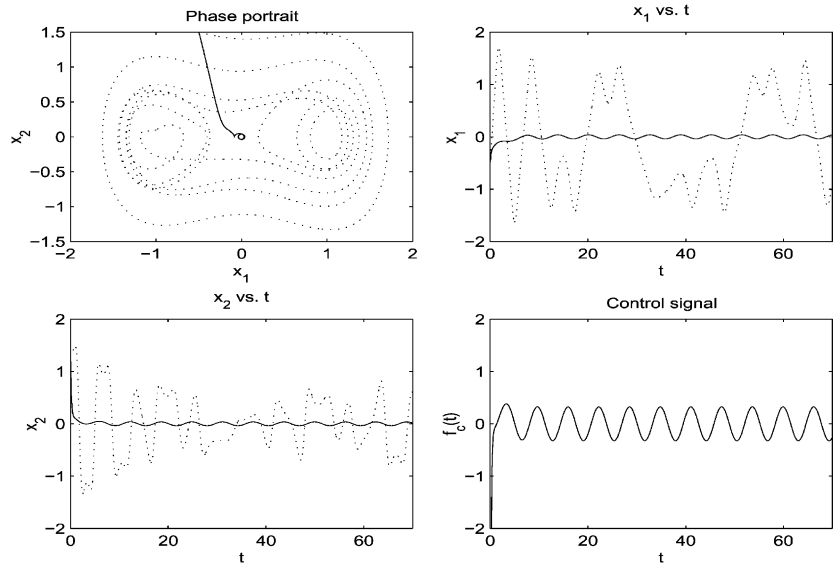

Fig. 1. Tracking trajectories of system (13) when $y_r \equiv 0$. Open-loop responses in dashed line and closed-loop responses in solid line.

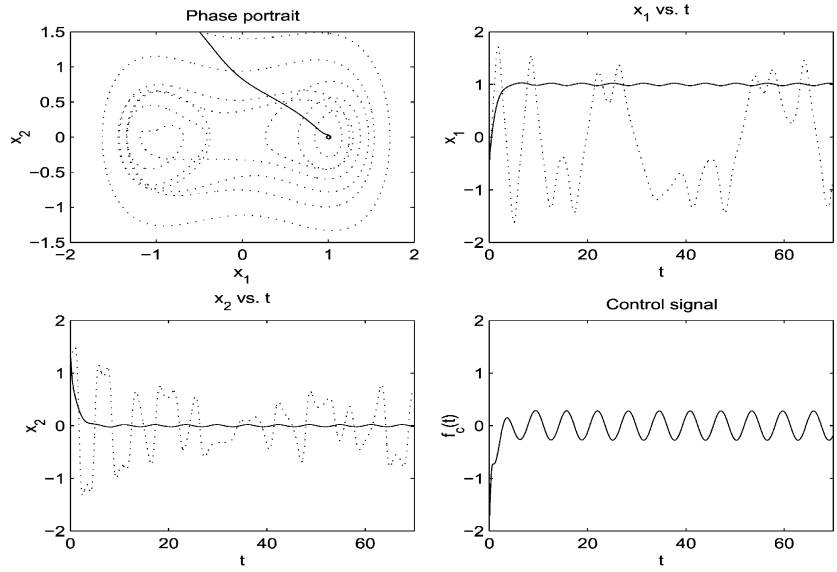

Fig. 2. Tracking trajectories of system (13) when $y_r \equiv 1$. Open-loop responses in dashed line and closed-loop responses in solid line.

tracking signal $y_r(t)$ (dashed line) and the controlled signal x_1 (solid line) to illustrate the good tracking of the desired reference signal. The performance index is $P_{r.m.s.,[0,70]} = 0.1269$. Also in this case $S_{r.m.s.,[0,70]} = 2.5115$. Of course, pretending to have a fast transient regime

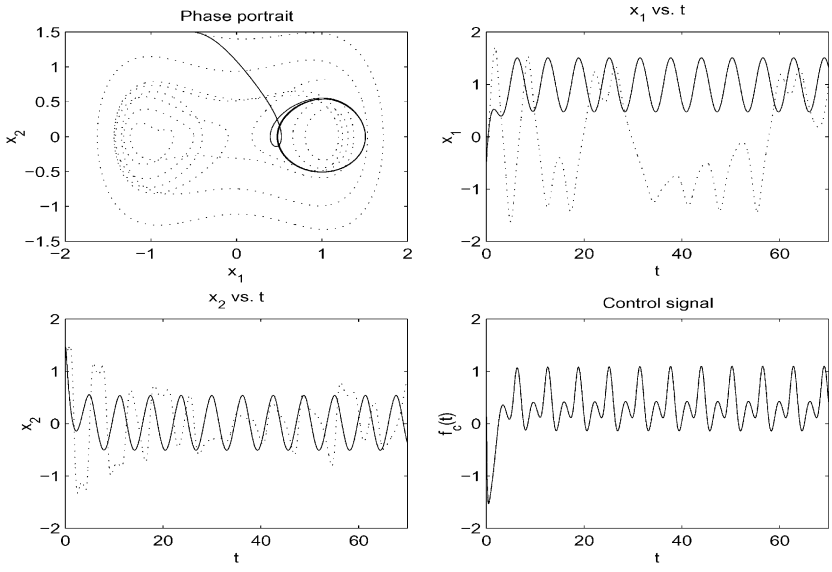

Fig. 3. Tracking trajectories of system (13) when $y_r(t) = 1 + 0.5\cos(t)$. Open-loop responses in dashed line and closed-loop responses in solid line.

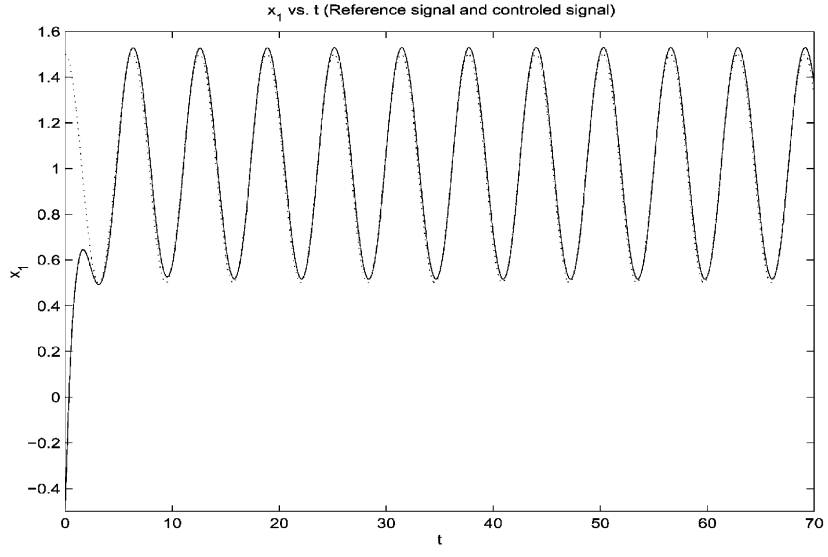

Fig. 4. Reference tracking signal $y_r(t) = 1 + 0.5\cos(t)$ in dashed line and closed-loop response of system (13) $x_1(t)$, in solid line.

to a capricious sustained oscillatory signal has the cost of having to apply a sustained high control action.

The data results for these three simulations are displayed in Table 1.

Table 1
Data results from simulations in Section 3 (Duffing oscillator: ($\|\cdot\|$ means $\|\cdot\|_{r.m.s.,[0,70]}$))

Target		Performance index	Error reduction (%)		Strength index
$y_r \equiv 0$	$\|\|z_1^{con}\|\| = 0.0460$ $\|\|z_1^{unc}\|\| = 0.8873$	$P_{r.m.s.,[0,70]} = 0.0518$	94.82	$\|\|f_c\|\| = 0.3479$ $\|\|e\|\| = 0.2129$	$S_{r.m.s.,[0,70]} = 1.6341$
$y_r \equiv 1$	$\|\|z_1^{con}\|\| = 0.1344$ $\|\|z_1^{unc}\|\| = 1.3798$	$P_{r.m.s.,[0,70]} = 0.0974$	90.26	$\|\|f_c\|\| = 0.2407$ $\|\|e\|\| = 0.2129$	$S_{r.m.s.,[0,30]} = 1.1306$
$y_r \equiv 1 + 0.5\cos(t)$	$\|\|z_1^{con}\|\| = 0.1825$ $\|\|z_1^{unc}\|\| = 1.4386$	$P_{r.m.s.,[0,30]} = 0.1269$	87.31	$\|\|f_c\|\| = 0.5343$ $\|\|e\|\| = 0.2129$	$S_{r.m.s.,[0,70]} = 2.5115$

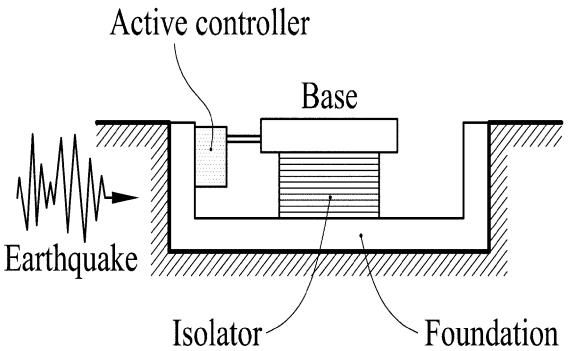

Fig. 5. Base isolation system.

4. Application: control of base isolation systems

4.1. System description and control design

In this section a one degree-of-freedom non-linear system which models a base isolation device as illustrated in Fig. 5 is considered. This system is the main component in base isolation schemes installed to supply passive and active protection in structures (like buildings) against earthquakes. The passive resistance is given by the physical characteristics of the isolator between the base and the foundation. The active resistance is given by a controller which produces forces generated by a feedback control law. Hybrid schemes by combining passive and active means have been proposed in recent years, attracting the interest of researchers from both structural and control engineering [20–22].

The model has the form

$$m\ddot{x} + c\dot{x} + F_s(x, t) = -ma(t) + f_c(t), \tag{14}$$

where x is the base displacement relative to the ground, m and c are the mass and the viscous damping coefficient, respectively, and $F_s(x, t)$ describes a non-linear restoring force. The excitation is supplied by the ground acceleration $a(t)$ and $f_c(t)$ is the force supplied by the active controller.

The purpose here is to design the control force by means of the backstepping control law presented in Section 2 with the aim of reducing the response of the system induced by the seismic acceleration.

Defining the state variables $(x_1, x_2) = (x, \dot{x})$ (14) may be written in the form

$$\begin{aligned} \dot{x}_1 &= x_2, \\ \dot{x}_2 &= -\frac{c}{m}x_2 - \frac{F_s(x_1,t)}{m} - a(t) + \frac{f_c(t)}{m}. \end{aligned} \tag{15}$$

For the control design, this system should have the structure assumed in Eqs. (1)–(3) and satisfy Assumptions 1–4 in Section 2. In this application mathematical description of the restoring force F_s is not considered a priori available for the control designer. Instead, for a number of time instants t_i $(i = 1, \ldots, N)$, the values of the displacement $x_1(t_i)$ and the corresponding restoring force $F_s(x_1(t_i), t_i)$ are known. This information can be available, for instance, from experimental input–output tests in which displacement and restoring force have been measured. Or it can be known by means of a physical constitutive model or a mathematical model which is considered as a "true" ideal description of a class of base isolation devices. Considering that the data set $(x_1(t_i), F_s(x_1(t_i), t_i))$ is available, an off-line identification procedure is performed to obtain an approximating function $F_s(x_1, t)$ with the structure adopted in Eq. (2).

More specifically, the idea is that it is possible to approximate the non-linear restoring force by an n order least-squares regression polynomial, that is, this function is assumed to have the following structure:

$$F_s(x,t) = \Psi(x) + R_e(x,t), \quad \Psi(x) \triangleq \delta_0^* + \delta_1^* \frac{x}{d} + \delta_2^* \left(\frac{x}{d}\right)^2 + \cdots + \delta_n^* \left(\frac{x}{d}\right)^n, \tag{16}$$

where $\Psi(x)$ is an n degree polynomial and $R_e(x,t)$ is a residual function. In the polynomial, d is a known constant with the dimension of a displacement. It is introduced so that all the coefficients δ_i^* have the same dimension (of a force). This representation of a restoring force lies within the class of the so-called non-parametric models [23–25]. In general, these models attempt to approximate unknown non-linear behaviours by functional expansions with appropriate coefficients, which are usually chosen through identification experiments. In Eq. (16), a simple polynomial plus a residual function is adopted as a description of the non-linearity. Its purpose here is not to give a precise model of the non-linearity, but to be used as a working model for the controller design. In fact, the coefficients δ_i and the function $R_e(x,t)$ do not need to be known exactly for the controller design, but must be bounded in the form $|R_e(x,t)| \leqslant \bar{R}_e$ for all x and $t \geqslant 0$, where $\bar{R}_e$ is a known positive constant.

Let $e_i(t_i)$ denote the errors between the fitted values and the "true" values

$$e_i = |F_s(x_1(t_i), t_i) - \Psi(x_1(t_i))|. \tag{17}$$

If the residual error $R_e(x_1, t) = F_s(x_1(t), t) - \Psi(x_1(t))$ of the least-squares approximation is a normally distributed random variable with mean $\mu_R = 0$ and variance σ_R^2, then a good estimation for σ_R^2 is given by

$$\sigma_R^2 = \frac{1}{N - (n+1)} \sum_{i=1}^{N} e_i^2, \tag{18}$$

(see, for more details, Ref. [26, Chapter 13]). In such a case, $3\sigma_R$ would be a good estimation for a bound $\bar{R}_e$ of $|R_e(x_1,t)|$. Since, in general, this will not be the case, the following estimation of $\bar{R}_e$ is adopted:

$$\bar{R}_e \triangleq \max(e_{max}, 3\sigma_R), \tag{19}$$

where $e_{max} = \max_{i=1,\ldots,N} e_i$.

By substituting the identified function $F_s(x_1,t)$ of Eq. (16) into Eq. (15), it can be written that

$$\begin{aligned} \dot{x}_1 &= x_2, \\ \dot{x}_2 &= \mathbf{\Phi}(x_1,x_2)^{\mathrm{T}}\mathbf{\Theta} + R(x_1,t) - a(t) + u(t) \end{aligned} \tag{20}$$

with

$$\mathbf{\Theta} = \left(\frac{cv}{m}, \delta_0, \delta_1, \delta_2, \ldots, \delta_n\right)^{\mathrm{T}}, \quad \mathbf{\Phi}(x_1,x_2) = -\left(\frac{x_2}{v}, 1, \frac{x_1}{d}, \frac{x_1^2}{d^2}, \ldots, \frac{x_1^n}{d^n}\right)^{\mathrm{T}},$$
$$\delta_i = \frac{\delta_i^*}{m}, \quad R(x_1,t) = \frac{R_e(x_1,t)}{m} \quad \text{and} \quad u(t) = \frac{f_c(t)}{m},$$

where v is a known constant which has the dimension of a velocity. It is introduced to have dimensionless variables in $\mathbf{\Phi}$ and coefficients of the same dimension in $\mathbf{\Theta}$.

Now model (20) has the same form as the one in Eq. (3). As for the Assumptions 1–4 in Section 2, consider that the mass m is known, while the damping coefficient c is unknown but lies within an interval $[0, c_{max}]$, where c_{max} is known. Now consider that the values of the constant vector $\mathbf{\Theta}_\delta = (\delta_0, \delta_1, \delta_2, \ldots, \delta_n)^{\mathrm{T}}$ obtained in the previous identification are only nominal values and assume that the "true" parameters are not precisely known by the control designer. This allows one to cope with some degree of uncertainty in the identification of the restoring force from the data as performed above. Thus, according to Assumption 2, the control design considers that the parameter vector $\mathbf{\Theta}$ is unknown but lies within a known sphere, which contains the nominal identified parameters. That is, $\|\mathbf{\Theta}_\delta\| \leqslant M_\delta$ for a known positive constant M_δ. Consequently, the following bound for vector $\mathbf{\Theta}$ is obtained:

$$\|\mathbf{\Theta}\| \leqslant \sqrt{\left(\frac{c_{max}v}{m}\right)^2 + M_\delta^2} \triangleq M. \tag{21}$$

For Assumption 3,

$$|R(x,t)| = \frac{|R_e(x,t)|}{m} \leqslant \frac{\bar{R}_e}{m} \triangleq \bar{R}. \tag{22}$$

Finally, according to Assumption 4, the seismic acceleration disturbance $a(t)$ is considered to be unknown, but bounded in the form $|a(t)| \leqslant A$, where A is a known positive constant. With this value, it is possible to obtain

$$r = \bar{R} + A, \tag{23}$$

which, together with M in Eq. (21), is needed in the control scheme (6)–(7).

The approach presented above is tested in the remainder of the paper. Since a real system is not available for a true implementation, the data set $(x_1(t_i), F_s(x_1(t_i), t_i))$ for fitting a restoring force function as considered above will be supplied by a mathematical model which is considered as the

"true" system. Two cases are considered. In the first one, the real restoring force is described by a high order polynomial function $F_s(x)$. In the second one, it is described by the well-known Bouc–Wen model [12,17,18], which represents a hysteretic restoring force by means of a differential equation.

4.2. Base isolation with high order non-linear stiffness

Duffing-type oscillators, such as the one in Eq. (12), have been used to describe restoring forces in such structural systems [12,13]. However, some works have reported that polynomial representations with terms beyond the cubic may be required to capture the essential behaviour of highly non-linear restoring forces in real physical structures [13,15,16]. Inspired by these works, in this section the adaptive backstepping control law presented in Section 2 will be applied to a model of a non-linear base isolation like the one in Eq. (14) in which the restoring force is a polynomial

$$m\ddot{x} + c\dot{x} + P(x) = -ma(t) + f_c(t),$$
$$P(x) = m\omega^2\left(x + \sum_{j=2}^{l} \delta_j x^j\right), \tag{24}$$

where ω, l, δ_j $(k = 1, \ldots, l)$ are uncertain parameters.

Numerical simulations assessing the efficiency of the control law are presented in the next section.

4.2.1. Simulation results

Consider system (24) with $l = 7$ and the following parameter values: mass $m = 156 \times 10^3$ kg, $\omega = 2\pi$ rad/s, damping $c = 2 \times 10^4$ Ns/m (which gives a 1% damping factor). Setting $k_i = m\omega^2\delta_i$, gives $k_1 = m\omega^2 = 6.1586 \times 10^6$ N/m, $k_2 = 1.7 \times 10^6$ N/m^2, $k_3 = 3.2 \times 10^6$ N/m^3, $k_4 = 4.8 \times 10^9$ N/m^4, $k_5 = 2.6 \times 10^{10}$ N/m^5, $k_6 = 1.3 \times 10^9$ N/m^6, $k_7 = 7.2 \times 10^{20}$ N/m^7. These parameters define the true system, which is not known for the control designer. The objective of the control is to keep the system response substantially reduced against an earthquake whose acceleration $a(t)$ is unknown but bounded by 1.2 m/s^2. Fig. 6 shows a prototype acceleration record (Taft's earthquake) which lies within this bound and will be used to perform numerical tests.

Prior to the design of the control law, the polynomial identification described in Section 4.1 has to be carried out. To do this, an open-loop simulation is performed, applying to system (24) a slow-varying excitation given by $a(t) = 1.5\cos(0.2t)$, which is a signal with a little more amplitude than the one expected to be controlled. A simulation time of 5 s, with 15 147 discrete time instants is taken for the identification, obtaining the values

$$x_1(t_i), \quad P(x_1(t_i)) = m\omega^2 x_1(t_i) + \sum_{j=2}^{7} k_j x_1^j(t_i) \quad \text{for } i = 1, \ldots, 15\,147.$$

The values of the constants d and v are determined from the open-loop identification as the maximum output (displacement and velocity, respectively) for the Taft's earthquake input. Thus taking $d = 0.03$ m and $v = 0.2$ m/s, the following third order least-squares regression polynomial

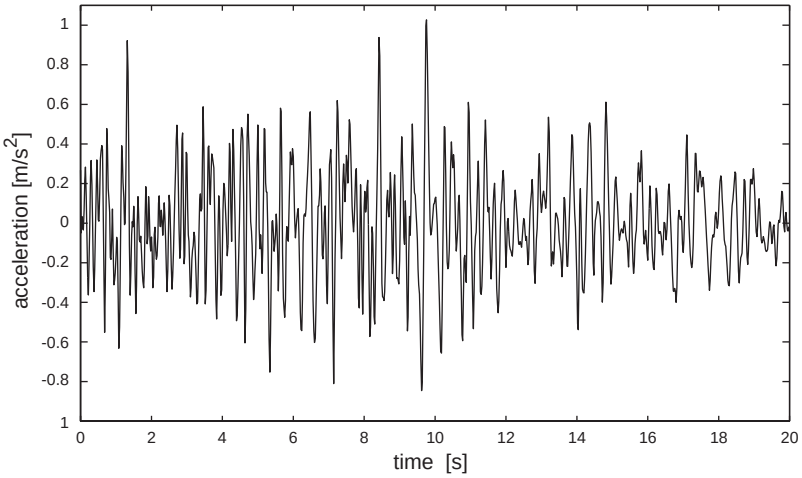

Fig. 6. Taft's earthquake acceleration signal.

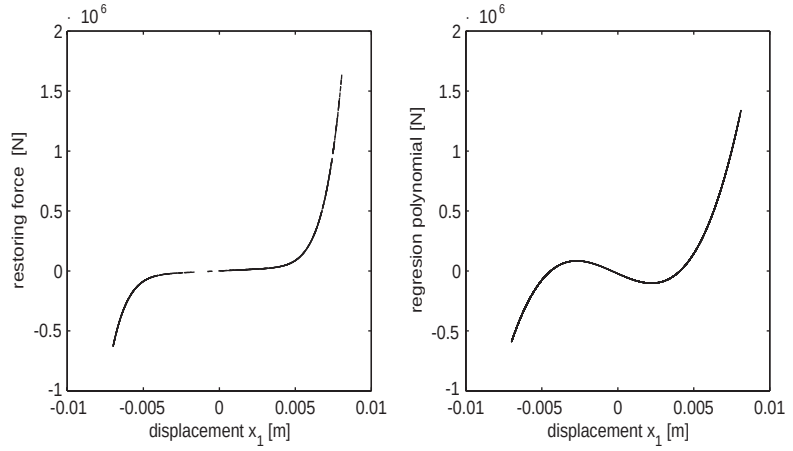

Fig. 7. Non-linear restoring force identification.

is obtained:

$$\Psi(x_1) = \left(-0.1458 - 10.8279\frac{x_1}{d} - 13.0085\left(\frac{x_1}{d}\right)^2 - 543.1181\left(\frac{x_1}{d}\right)^3\right)m, \tag{25}$$

with a maximum error $e_{max} = 2.3248$ m and a variance error $\sigma_R = 0.5381$ m, so that $\bar{R}_e = 2.3248$ m. Fig. 7 displays the results of the identification by comparing the behaviour of the "true" system restoring force and the identified polynomial.

For the control law implementation, the values of the uncertainty bounds r and M in Eqs. (6) and (7) need to be set. Assuming that the excitation is bounded in the form $|a(t)| \leqslant A = 1.2$, then $r = \bar{R} + A = 3.5248$. Consider $c^{(nom)} = 2 \times 10^4$ and the vector $\boldsymbol{\Theta}_{\delta}^{(nom)} = (-0.1458, -10.8279,$

$13.0085, 543.1181)^{\mathrm{T}}$ with the parameters identified in Eq. (25) as nominal model values. Compute $\|\boldsymbol{\Theta}_{\delta}^{(nom)}\| = 543.3818$. Now, some uncertainty margins to these parameters are included, so that the real values c and $\boldsymbol{\Theta}_{\delta}$, which are unknown for the control law, have the following bounds:

$$0 \leqslant c \leqslant c_{max} = 2c^{(nom)} = 4 \times 10^4, \quad \|\boldsymbol{\Theta}_{\delta}\| \leqslant M_{\delta} = 2\|\boldsymbol{\Theta}_{\delta}^{(nom)}\| = 1.0868 \times 10^3.$$

These bounds allow one to cope with some degree of uncertainty in the true system model (24) and errors in the performed identification. With these values the following is obtained:

$$M = \sqrt{\left(\frac{c_{max}v}{m}\right)^2 + M_{\delta}^2} = 1.0868 \times 10^3 \ \mathrm{m/s^2}.$$

After some numerical experiments, the following design parameters are chosen: $c_1 = 100$, $c_2 = 5$, $\varepsilon_1 = 0.01$, $\varepsilon_2 = 0.1$, $\bar{\sigma} = 1$ and $\boldsymbol{\Gamma} = \mathbf{I}_5$ (the 5×5 identity matrix). For the parameter adaptive law in Eq. (6), the following initial parameter vector $\hat{\boldsymbol{\Theta}}_0$ has been chosen:

$$\hat{\boldsymbol{\Theta}}_0 = \left(\frac{c_{max}v}{m}, \boldsymbol{\Theta}_{\delta}^{(nom)T}\right)^{\mathrm{T}}.$$

Starting at time 0 with these values, the adaptive law in Eq. (6) updates on-line new values of these parameters.

The system is subjected to the Taft earthquake excitation, whose acceleration is plotted in Fig. 6. Since the control objective is to mitigate the seismic displacement response of the system, the target for x_1 is set to $y_r = 0$.

Fig. 8 shows the behaviour of system (24) both in the case without control and with the backstepping active control in operation. The phase portrait and the time histories of the displacement and the velocity exhibit a significant reduction of the controlled response in comparison to the open-loop response. After $t = 20$ s, the excitation stops and the uncontrolled

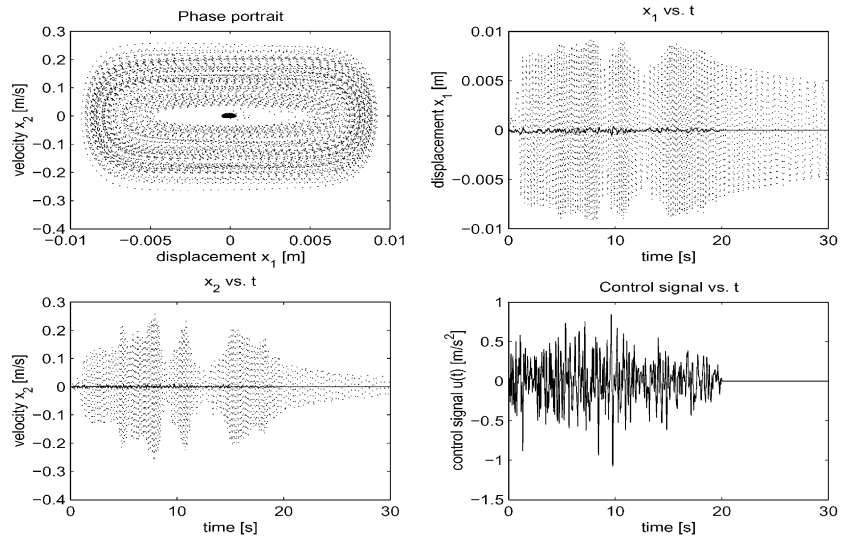

Fig. 8. Tracking trajectories of system (24) when $y_r \equiv 0$. Open-loop responses in dashed line and closed-loop responses in solid line.

Table 2
Data results from simulations in Section 4.2 ($\|\cdot\|_T$ means $\|\cdot\|_{r.m.s.,[0,T]}$)

Time		Performance index	Error reduction (%)		Strength index
$T = 20$ s	$\|z_1^{con}\|_{20} = 1.5135 \times 10^{-4}$			$\|u\|_{20} = 0.2571$	
	$\|z_1^{unc}\|_{20} = 0.0050$	$P_{r.m.s.,[0,20]} = 0.0303$	96.97	$\|e\|_{20} = 0.2503$	$S_{r.m.s.,[0,20]} = 1.0272$
$T = 30$ s	$\|z_1^{con}\|_{30} = 1.2371 \times 10^{-4}$			$\|u\|_{30} = 0.2099$	
	$\|z_1^{unc}\|_{30} = 0.0046$	$P_{r.m.s.,[0,30]} = 0.0269$	97.31	$\|e\|_{30} = 0.2044$	$S_{r.m.s.,[0,30]} = 1.0269$

case corresponds to free vibration response. The open-loop system exhibits a low damping behaviour. On the contrary, the control drives a fast response towards the neighbourhood of zero, thus introducing a significant damping effect into the system. The performance index at 20 s (when the earthquake finishes), and at 30 s are given by $P_{r.m.s.,[0,20]} = 0.0303$, and $P_{r.m.s.,[0,30]} = 0.0269$, respectively, which gives a regulation error reduction for x_1 of 96.97% and 97.31% respectively. The strength index at 20 s is $S_{r.m.s.,[0,20]} = 1.0249$, and at 30 s is $S_{r.m.s.,[0,30]} = 1.0249$. This means that to reduce 97% (in average) vibration, the control signal has to be of almost the same size of the external excitation. The data results of this simulation are summarized in Table 2.

Fig. 8 also shows the time history of the control signal $u(t)$. Physically, this signal is an acceleration. Its pattern seems reasonable in comparison with the seismic excitation acceleration in Fig. 6.

4.3. Base isolation with hysteretic behaviour

Hysteretic restoring forces are very common when dealing with structural systems, in particular, in base isolation schemes. In this section, the dynamics of the base isolation device (14) is represented in the form

$$\begin{aligned} &m\ddot{x} + c\dot{x} + H(x,t) = -ma(t) + f_c(t), \\ &H(x,t) = \alpha k x(t) + (1-\alpha) k D z(t), \end{aligned} \tag{26}$$

where $H(x,t)$ describes a non-linear hysteretic uncertain restoring force as the superposition of an elastic component $\alpha k x(t)$ and a hysteretic component $(1-\alpha)kDz(t)$. This component involves a non-dimensional auxiliary variable $z(t)$ which is the solution of the following non-linear first order differential equation:

$$\dot{z} = D^{-1}[A\dot{x} - \beta|\dot{x}|\,|z|^{n-1}z - \gamma\dot{x}|z|^n]. \tag{27}$$

In this equation, $D > 0$ is the yield constant displacement and $\alpha \in [0,1]$ is the post to pre-yielding stiffness ratio, A, β and γ are non-dimensional parameters which control the shape and the size of the hysteresis loop, while n is an integer that governs the smoothness of the transition from elastic to plastic response. The above hysteretic force description is the so called Bouc-Wen model [17], which belongs to the class of differential hysteretic models and has been widely used in structural dynamics, particularly to describe rubber bearing base isolation schemes [18].

4.3.1. Simulation results

Consider systems (26)–(27) with the following parameter values: mass $m = 156 \times 10^3$ kg, stiffness $k = 6 \times 10^6$ N/m, damping $c = 2 \times 10^4$ Ns/m, $\alpha = 0.6$, $D = 0.6$ m, $A = 1$, $\beta = 0.5$, $\gamma = 0.5$ and $n = 3$.

As in the previous example, the purpose here is to check the control efficiency against the action of an earthquake whose acceleration is roughly bounded by 1.2 m/s^2. Thus, for the polynomial identification described in Section 4.1, an open-loop simulation of the response of systems (26)–(27) is done introducing a slow-varying excitation given by $a(t) = 1.5\cos(0.2t)$. Take $z(0) = 0$ and a simulation time of 100 s, with 8226 discrete time instants for the identification, obtaining the following values:

$$x_1(t_i), \quad H(x_1(t_i), t_i) = \alpha k x_1(t_i) + (1-\alpha)kDz_i(t) \quad \text{for } i = 1, \ldots, 8226.$$

The values of d and v are determined from the open-loop identification as the maximum output (displacement and velocity, respectively) for the Taft's earthquake input. This gives $d = 0.03$ m and $v = 0.2$ m/s. The following third order least-squares regression polynomial is obtained:

$$\Psi(x_1) = \left(-0.02 + 1.14\frac{x_1}{a} - 0.001\left(\frac{x_1}{a}\right)^2 - 0.024\left(\frac{x_1}{a}\right)^3\right)m, \tag{28}$$

with a maximum error $e_{max} = 0.4365$ m and a variance error $\sigma_R = 0.1446$ m, so that $\bar{R}_e = 0.4365$ m.

Fig. 9 displays the results of the hysteresis identification, by comparing the hysteretic behaviour of the Bouc-Wen model (''true'' system) and the identified polynomial.

Assuming that the excitation is bounded in the form $|a(t)| \leqslant A = 1.2$, then $r = \bar{R} + A = 1.6365$. Now consider $c^{(nom)} = 2 \times 10^4$ and the vector

$$\boldsymbol{\Theta}_\delta^{(nom)} = (-0.02, 1.14, -0.001, -0.024)^{\mathrm{T}},$$

with the parameters identified in Eq. (28) as nominal model values. Compute $\|\boldsymbol{\Theta}_\delta^{(nom)}\| = 1.14$. As in the previous example, it is assumed that the above values are only ideal nominal parameters,

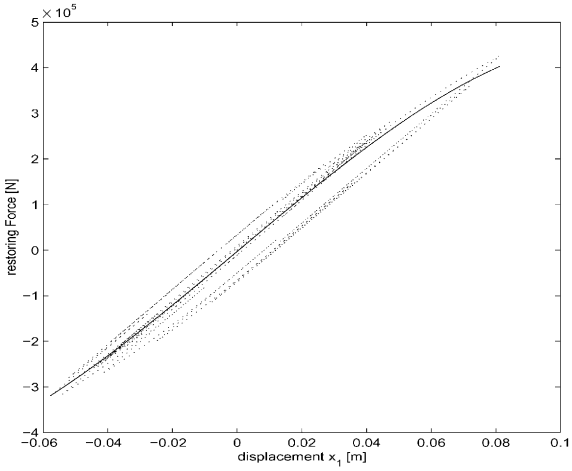

Fig. 9. Hysteresis identification: hysteretic cycles (dashed line) and regression polynomial (solid line).

and uncertainty bounds are introduced by considering $c_{max} = 2c^{(nom)} = 4 \times 10^4$ and $M_\delta = 2\|\mathbf{\Theta}_\delta^{(nom)}\| = 2.28$. With these values the following is obtained:

$$M = \sqrt{\left(\frac{c_{max} v}{m}\right)^2 + M_\delta^2} = 2.28 \text{ m/s}^2.$$

The following design parameters are chosen: $c_1 = 5$, $c_2 = 5$, $\varepsilon_1 = 0.01$, $\varepsilon_2 = 0.1$, $\bar{\sigma} = 1$ and $\mathbf{\Gamma} = \mathbf{I}_5$. The parameter adaptive law in Eq. (6) is initialized at: $\hat{\mathbf{\Theta}}_0 = (c_{max} v/m, \mathbf{\Theta}_\delta^{(nom)T})^{\mathrm{T}}$. The control objective is to mitigate the seismic displacement response of the system, hence the target for x_1 is set to $y_r = 0$. The system is subjected to the Taft earthquake excitation (Fig. 6).

The system behaviour is shown in Fig. 10, both in the case without control and with active control. A significant reduction can be observed due to the control (solid lines). When the excitation stops at $t = 20$ s, the uncontrolled system shows a low damped-free vibration response, while the controlled system behaves highly damped, as already observed in the previous example in Fig. 1. The time history of the control acceleration signal in Fig. 10 also shows a reasonable behaviour in comparison with the seismic acceleration excitation in Fig. 6.

After 20 s (at the end of the earthquake), the performance index is given by $P_{r.m.s.,[0,20]} = 0.0430$, which gives a reduction of 95.70% in the regulation error for x_1, and after 30 s $P_{r.m.s.,[0,30]} = 0.0403$, which gives a reduction of 95.97%. The strength indices are $S_{r.m.s.,[0,20]} = 0.8905$ and $S_{r.m.s.,[0,30]} = 0.8904$. All the data results for this simulation are given in Table 3.

Note that the parameter r has been obtained experimentally. If bigger values of r are considered (for instance, to have a more conservative estimation of the uncertainties), the control action becomes stronger. New simulations have been obtained taking $r = 2$ and $r = 2.5$, which represents an increase of 22.21% and 50%, respectively, of the uncertainty with respect to the case $r =$

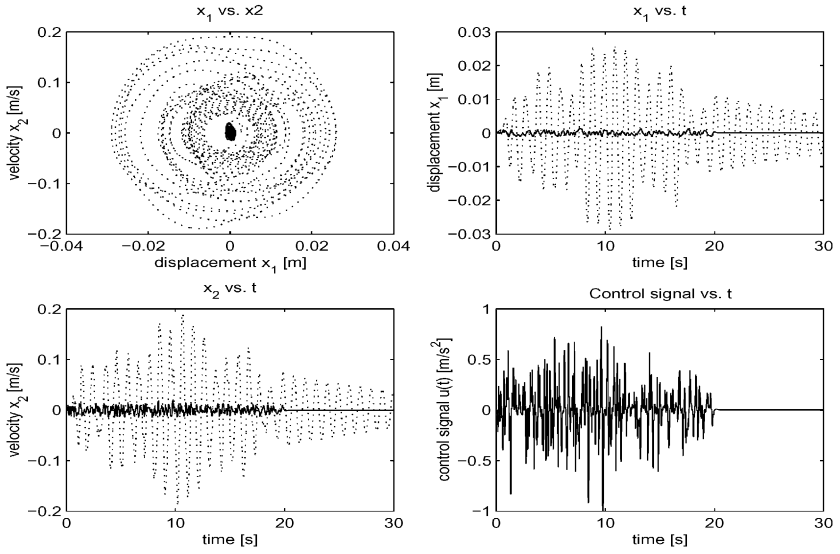

Fig. 10. Tracking trajectories of system (26) when $y_r \equiv 0$. Open-loop responses in dashed line and closed-loop responses in solid line.

Table 3
Data results from simulations in Section 4.3, for the case $r = 1.6365$ (Bouc–Wen oscillator: Case $r = 1.6365$ ($\|\cdot\|_T$ means $\|\cdot\|_{r.m.s.,[0,T]}$))

Time		Performance index	Error reduction (%)		Strength index
$T = 20$ s	$\|z_1^{con}\|_{20} = 5.3701 \times 10^{-4}$			$\|u\|_{20} = 0.2229$	
	$\|z_1^{unc}\|_{20} = 0.0125$	$P_{r.m.s.,[0,20]} = 0.0430$	95.70	$\|e\|_{20} = 0.2503$	$S_{r.m.s.,[0,20]} = 0.8905$
$T = 30$ s	$\|z_1^{con}\|_{30} = 4.3964 \times 10^{-4}$			$\|u\|_{30} = 0.1820$	
	$\|z_1^{unc}\|_{30} = 0.0109$	$P_{r.m.s.,[0,30]} = 0.0403$	95.97	$\|e\|_{30} = 0.2044$	$S_{r.m.s.,[0,30]} = 0.8904$

Table 4
Data results from simulations in Section 4.3, for the case $r = 2$ (Bouc–Wen oscillator: Case $r = 2$ ($\|\cdot\|_T$ means $\|\cdot\|_{r.m.s.,[0,T]}$))

Time		Performance index	Error reduction (%)		Strength index
$T = 20$ s	$\|z_1^{con}\|_{20} = 4.3627 \times 10^{-4}$			$\|u\|_{20} = 0.2311$	
	$\|z_1^{unc}\|_{20} = 0.0125$	$P_{r.m.s.,[0,20]} = 0.0349$	96.51	$\|e\|_{20} = 0.2503$	$S_{r.m.s.,[0,20]} = 0.9233$
$T = 30$ s	$\|z_1^{con}\|_{30} = 3.5723 \times 10^{-4}$			$\|u\|_{30} = 0.1887$	
	$\|z_1^{unc}\|_{30} = 0.0109$	$P_{r.m.s.,[0,30]} = 0.0328$	96.72	$\|e\|_{30} = 0.2044$	$S_{r.m.s.,[0,30]} = 0.9232$

Table 5
Data results from simulations in Section 4.3, for the case $r = 2.5$ (Bouc–Wen oscillator: Case $r = 2.5$ ($\|\cdot\|_T$ means $\|\cdot\|_{r.m.s.,[0,T]}$))

Time		Performance index	Error reduction (%)		Strength index
$T = 20$ s	$\|z_1^{con}\|_{20} = 3.4340 \times 10^{-4}$			$\|u\|_{20} = 0.2379$	
	$\|z_1^{unc}\|_{20} = 0.0125$	$P_{r.m.s.,[0,20]} = 0.0275$	97.25	$\|e\|_{20} = 0.2503$	$S_{r.m.s.,[0,20]} = 0.9505$
$T = 30$ s	$\|z_1^{con}\|_{30} = 2.8122 \times 10^{-4}$			$\|u\|_{30} = 0.1942$	
	$\|z_1^{unc}\|_{30} = 0.0109$	$P_{r.m.s.,[0,30]} = 0.0258$	97.42	$\|e\|_{30} = 0.2044$	$S_{r.m.s.,[0,30]} = 0.9501$

1.6365. The reduction of the regulation errors for x_1, at 20 s, and at 30 s (respectively) are of 96.51% and 96.72% (respectively) for the $r = 2$ case, and of 97.25% and 97.42% (respectively) for the $r = 2.5$ case. The results for these numerical experiments are summarized in Tables 4 and 5, respectively.

Setting $r = 2$, the strength indices at 20 and 30 s have an increase of only 3.68% in both cases with respect the same indices when $r = 1.6365$.

In the case $r = 2.5$, the strength indices at 20 and 30 s have an increase of only 6.74% and 6.70%, (respectively) with respect to the same indices when $r = 1.6365$.

Table 6 summarizes the compared data results for the experiments in the above three cases.

Table 6
Comparison results for simulations in Section 4.3, for the cases $r = 2$, and $r = 2.5$ with respect to $r = 1.6365$ (Bouc–Wen oscillator: Comparison results respect to $r_0 \triangleq 1.6365$)

r	Added uncertainty respect to r_0	Performance	Error reduction (%)	Strength	Increase of S respect to r_0
$r_0 = 1.6365$		$P_{r.m.s.,[0,20]} = 0.0430$ $P_{r.m.s.,[0,30]} = 0.0403$	95.70 95.97	$S_{r.m.s.,[0,20]} = 0.8905$ $S_{r.m.s.,[0,30]} = 0.8904$	
$r = 2$	22.21%	$P_{r.m.s.,[0,20]} = 0.0349$ $P_{r.m.s.,[0,30]} = 0.0328$	96.51 96.72	$S_{r.m.s.,[0,20]} = 0.9233$ $S_{r.m.s.,[0,30]} = 0.9232$	3.68% 3.68%
$r = 2.5$	50%	$P_{r.m.s.,[0,20]} = 0.0275$ $P_{r.m.s.,[0,30]} = 0.0258$	97.25 97.42	$S_{r.m.s.,[0,20]} = 0.9505$ $S_{r.m.s.,[0,30]} = 0.9501$	6.74% 6.70%

5. Conclusions

This paper has presented a backstepping-based robust controller for a class of one-degree-of-freedom non-linear systems. For the control design, it is assumed that the non-linear behaviour can be described by a nominal function plus a remainder. The coefficients of the nominal and the residual function do not need to be known for the controller design. Indeed, an adaptive law is included in the control to estimate these coefficients on-line.

The behaviour of the closed loop is such that the response variables of the controlled system are globally uniformly ultimately bounded and they can be made arbitrarily small by an appropriate choice of design parameters. Both the transient and the asymptotic performance depend explicitly on the design parameters. Since decreasing the ultimate bound of the controlled response requires increasing the control action, a trade-off between a desired response reduction and a reasonable control level has to be judiciously considered.

The proposed control scheme has been tested in three different cases. In the first case the states of an uncertain Duffing oscillator, which exhibits a chaotic motion regime, are driven arbitrarily close either to a steady state or to a periodic orbit. In comparison with other methods usually applied to suppress "chaotic" motions, the backstepping approach developed in this work permits some control also on the transient performance. In the first example, however, this good behaviour of the transient performance is reached at expense of a high control action in comparison with the external excitation input.

The second and third applications refer to the control of oscillators appearing as models for non-linear base isolation devices. Since these models are based on differential equations with unknown parameters, a regression-based identification procedure has been proposed to obtain "experimentally" an approximation of the theoretical non-linear behaviour within the functional framework of the control scheme. The discrepancies between the identified non-linearity and the theoretical one are lumped in the uncertain coefficients of the polynomial and the residual function.

In order to test the efficiency of the control in this framework, two different types of non-linearities have been considered. One of the models is given by a seven order polynomial restoring

force and the other corresponds to a hysteretic system described by the Bouc-Wen model. Both systems are subjected to an earthquake excitation. The numerical results show that the combination of this uncertain description of the non-linearities and the backstepping adaptive control law is satisfactory in that the response induced by the seismic action is significantly reduced. These results are encouraging towards the applicability of the control scheme proposed in this paper. In effect, both the Bouc-Wen model and the other non-parametric approximations are widely used in structural dynamics, particularly in base isolation schemes where non-linear and hysteretic behaviours pose challenging problems for designing active control systems.

Acknowledgements

This work has been supported by the spanish Ministry of Science and Technology through the CICYT Grant DPI2002-04018-C02-01. V. Mañosa is also partially supported by the Government of Catalonia's Grant 2001SGR-00173. F. Ikhouane is supported by the "Ramón y Cajal" program. The authors acknowledge the anonymous referee's comments that have helped to improve the manuscript.

Appendix A. Proofs of the main results

Proof of Theorem 1. Consider the Lyapunov's function candidate

$$V(z_1, z_2, \tilde{\boldsymbol{\Theta}}) \triangleq \tfrac{1}{2} z_1^2 + \tfrac{1}{2} z_2^2 + \tfrac{1}{2} \tilde{\boldsymbol{\Theta}}^{\mathrm{T}} \boldsymbol{\Gamma}^{-1} \tilde{\boldsymbol{\Theta}}, \tag{A.1}$$

where $\tilde{\boldsymbol{\Theta}} = \boldsymbol{\Theta} - \hat{\boldsymbol{\Theta}}$. Since $\dot{\tilde{\boldsymbol{\Theta}}}^{\mathrm{T}} \boldsymbol{\Gamma}^{-1} \tilde{\boldsymbol{\Theta}} \in \mathbb{R}$, we have that $\frac{1}{2} \dot{\tilde{\boldsymbol{\Theta}}}^{\mathrm{T}} \boldsymbol{\Gamma}^{-1} \tilde{\boldsymbol{\Theta}} + \frac{1}{2} \tilde{\boldsymbol{\Theta}}^{\mathrm{T}} \boldsymbol{\Gamma}^{-1} \dot{\tilde{\boldsymbol{\Theta}}} = \tilde{\boldsymbol{\Theta}}^{\mathrm{T}} \boldsymbol{\Gamma}^{-1} \dot{\tilde{\boldsymbol{\Theta}}}$, hence the orbital derivative of V is given by

$$\dot{V} = z_1 \dot{z}_1 + z_2 \dot{z}_2 + \tilde{\boldsymbol{\Theta}}^{\mathrm{T}} \boldsymbol{\Gamma}^{-1} \dot{\tilde{\boldsymbol{\Theta}}}. \tag{A.2}$$

Using that $\dot{z}_1 = z_2 - c_1 z_1$, $\dot{\alpha}_1 = -c_1 z_2 + c_1^2 z_1 + \ddot{y}_r$ and $\dot{z}_2 = \boldsymbol{\Phi}^{\mathrm{T}} \boldsymbol{\Theta} + R + \mathrm{e} + u + c_1 x_2 - c_1 \dot{y}_r - \ddot{y}_r$, the following is obtained:

$$\dot{V} = z_1 (z_2 - c_1 z_1) + z_2 (\boldsymbol{\Phi}^{\mathrm{T}} \boldsymbol{\Theta} + R + \mathrm{e} + u + c_1 x_2 - c_1 \dot{y}_r - \ddot{y}_r) + \tilde{\boldsymbol{\Theta}}^{\mathrm{T}} \boldsymbol{\Gamma}^{-1} \dot{\tilde{\boldsymbol{\Theta}}}. \tag{A.3}$$

Choosing the control law defined by Eq. (6) and using the fact that $\boldsymbol{\Phi}^{\mathrm{T}} \boldsymbol{\Theta} = \boldsymbol{\Phi}^{\mathrm{T}} (\tilde{\boldsymbol{\Theta}} + \hat{\boldsymbol{\Theta}})$, from Eq. (A.3)

$$\dot{V} = -c_1 z_1^2 - c_2 z_2^2 - z_2 \mathrm{sg}(z_2) \mathrm{cf}(|r z_2|) r + z_2 \boldsymbol{\Phi}^{\mathrm{T}} \tilde{\boldsymbol{\Theta}} + \tilde{\boldsymbol{\Theta}}^{\mathrm{T}} \boldsymbol{\Gamma}^{-1} \dot{\tilde{\boldsymbol{\Theta}}} + z_2 (R + \mathrm{e}).$$

Observe that $z_2 \boldsymbol{\Phi}^{\mathrm{T}} \tilde{\boldsymbol{\Theta}} + \tilde{\boldsymbol{\Theta}}^{\mathrm{T}} \boldsymbol{\Gamma}^{-1} \dot{\tilde{\boldsymbol{\Theta}}} = \tilde{\boldsymbol{\Theta}}^{\mathrm{T}} \boldsymbol{\Gamma}^{-1} (\dot{\tilde{\boldsymbol{\Theta}}} + \boldsymbol{\Gamma} \boldsymbol{\Phi} z_2)$. Choosing the parameter estimate law defined by Eq. (7), gives $\tilde{\boldsymbol{\Theta}}^{\mathrm{T}} \boldsymbol{\Gamma}^{-1} (\dot{\tilde{\boldsymbol{\Theta}}} + \boldsymbol{\Gamma} \boldsymbol{\Phi} z_2) = \sigma_{\Theta}(\|\hat{\boldsymbol{\Theta}}\|) \tilde{\boldsymbol{\Theta}}^{\mathrm{T}} \hat{\boldsymbol{\Theta}}$, and therefore

$$\dot{V} = -c_1 z_1^2 - c_2 z_2^2 - z_2 \mathrm{sg}(z_2) \mathrm{cf}(|r z_2|) r + \sigma_{\Theta}(\|\hat{\boldsymbol{\Theta}}\|) \tilde{\boldsymbol{\Theta}}^{\mathrm{T}} \hat{\boldsymbol{\Theta}} + z_2 (R + \mathrm{e}). \tag{A.4}$$

Now consider the term $\Delta_1 \triangleq z_2 (R + \mathrm{e} - \mathrm{sg}(z_2) \mathrm{cf}(|r z_2|) r)$ appearing in Eq. (A.4). First observe that if $|z_2| > \varepsilon_2/(1 + r) + 2\varepsilon_1/r$, then $\mathrm{sg}(z_2) = \mathrm{sign}(z_2)$, and $\mathrm{cf}(|r z_2|) = 1$, hence $\Delta_1 = (R + \mathrm{e}) z_2 - r|z_2| \leqslant 0$, since $|R + \mathrm{e}| \leqslant r$.

On the other hand, if $|z_2|<\varepsilon_2/(1+r)+2\varepsilon_1/r$, and since $\mathrm{cf}(|rz_2|)\leqslant 1$ and $\mathrm{sg}(z_2)\leqslant 1$, then

$$\begin{aligned}|\Delta_1| &\leqslant |z_2|(|R+\mathrm{e}|+|\mathrm{sg}(z_2)\mathrm{cf}(|rz_2|)r|)\\ &\leqslant 2r|z_2|\leqslant 2r(\varepsilon_2/(1+r)+2\varepsilon_1/r)\\ &\leqslant 2(r\varepsilon_2/(1+r)+2\varepsilon_1)\leqslant 2\varepsilon_2+4\varepsilon_1.\end{aligned}$$

Hence, in any case $\Delta_1\leqslant 2\varepsilon_2+4\varepsilon_1$, and therefore

$$\dot{V}=-c_1z_1^2-c_2z_2^2+\sigma_\Theta(\|\hat{\boldsymbol{\Theta}}\|)\tilde{\boldsymbol{\Theta}}^{\mathrm{T}}\hat{\boldsymbol{\Theta}}+2\varepsilon_2+4\varepsilon_1. \tag{A.5}$$

Now consider the term $\Delta_2\triangleq\sigma_\Theta(\|\hat{\boldsymbol{\Theta}}\|)\tilde{\boldsymbol{\Theta}}^{\mathrm{T}}\hat{\boldsymbol{\Theta}}$ appearing in Eq. (A.5). As shown in the proof of Theorem 2, Δ_2 is always negative. But for this purpose, at this point one need to use a more conservative estimation. On one hand, if $\|\hat{\boldsymbol{\Theta}}\|\geqslant 2M$ then $\sigma_\Theta(\|\hat{\boldsymbol{\Theta}}\|)=\bar{\sigma}$ (from now on, denote $\sigma_\Theta\triangleq\sigma_\Theta(\|\hat{\boldsymbol{\Theta}}\|)$). So using Assumption 2;

$$\begin{aligned}\sigma_\Theta\tilde{\boldsymbol{\Theta}}^{\mathrm{T}}\hat{\boldsymbol{\Theta}} &= \sigma_\Theta\tilde{\boldsymbol{\Theta}}^{\mathrm{T}}(\boldsymbol{\Theta}-\tilde{\boldsymbol{\Theta}})=\sigma_\Theta(\tilde{\boldsymbol{\Theta}}^{\mathrm{T}}\boldsymbol{\Theta}-\|\tilde{\boldsymbol{\Theta}}\|^2)\leqslant\bar{\sigma}(M\|\tilde{\boldsymbol{\Theta}}\|-\|\tilde{\boldsymbol{\Theta}}\|^2)\\ &= \bar{\sigma}\big(M\|\tilde{\boldsymbol{\Theta}}\|-\tfrac{1}{4}\|\tilde{\boldsymbol{\Theta}}\|^2-\tfrac{3}{4}\|\tilde{\boldsymbol{\Theta}}\|^2\big)=\bar{\sigma}\left(-\left[\frac{\|\tilde{\boldsymbol{\Theta}}\|}{2}-M\right]^2+M_{\boldsymbol{\Theta}}^2-\tfrac{3}{4}\|\tilde{\boldsymbol{\Theta}}\|^2\right)\\ &\leqslant \bar{\sigma}M_{\boldsymbol{\Theta}}^2-\tfrac{3}{4}\bar{\sigma}\|\tilde{\boldsymbol{\Theta}}\|^2.\end{aligned}$$

On the other hand, if $\|\hat{\boldsymbol{\Theta}}\|\leqslant 2M$ then $\|\tilde{\boldsymbol{\Theta}}\|=\|\boldsymbol{\Theta}-\hat{\boldsymbol{\Theta}}\|\leqslant\|\boldsymbol{\Theta}\|+\|\hat{\boldsymbol{\Theta}}\|\leqslant 3M$. Hence

$$\begin{aligned}\sigma_\Theta\tilde{\boldsymbol{\Theta}}^{\mathrm{T}}\hat{\boldsymbol{\Theta}} &\leqslant \bar{\sigma}(\|\tilde{\boldsymbol{\Theta}}\|\,\|\boldsymbol{\Theta}\|-\|\tilde{\boldsymbol{\Theta}}\|^2)=\bar{\sigma}\big(\|\tilde{\boldsymbol{\Theta}}\|\,\|\boldsymbol{\Theta}\|-\|\tilde{\boldsymbol{\Theta}}\|^2-\tfrac{3}{4}\|\tilde{\boldsymbol{\Theta}}\|^2+\tfrac{3}{4}\|\tilde{\boldsymbol{\Theta}}\|^2\big)\\ &\leqslant \bar{\sigma}\big(\|\tilde{\boldsymbol{\Theta}}\|\,\|\boldsymbol{\Theta}\|-\tfrac{3}{4}\|\tilde{\boldsymbol{\Theta}}\|^2+\tfrac{3}{4}\|\tilde{\boldsymbol{\Theta}}\|^2\big)\leqslant\bar{\sigma}\big(3M^2+\tfrac{3}{4}9M^2\big)-\tfrac{3}{4}\bar{\sigma}\|\tilde{\boldsymbol{\Theta}}\|^2\\ &= \tfrac{39}{4}\bar{\sigma}M^2-\tfrac{3}{4}\bar{\sigma}\|\tilde{\boldsymbol{\Theta}}\|^2.\end{aligned}$$

In summary, $\Delta_2\leqslant\frac{39}{4}\bar{\sigma}M^2-\frac{3}{4}\bar{\sigma}\|\tilde{\boldsymbol{\Theta}}\|^2$, and then from Eq. (A.5) the following is obtained:

$$\begin{aligned}\dot{V} &\leqslant -c_1z_1^2-c_2z_2^2-\tfrac{3}{4}\bar{\sigma}\|\tilde{\boldsymbol{\Theta}}\|^2+\tfrac{39}{4}\bar{\sigma}M^2+2\varepsilon_2+4\varepsilon_1\\ &\leqslant -\min\big(c_1,c_2,\tfrac{3}{4}\bar{\sigma}\big)(z_1^2+z_2^2+\|\tilde{\boldsymbol{\Theta}}\|^2)+\tfrac{39}{4}\bar{\sigma}M^2+2\varepsilon_2+4\varepsilon_1.\end{aligned} \tag{A.6}$$

Notice that

$$V\leqslant\tfrac{1}{2}z_1^2+\tfrac{1}{2}z_2^2+\tfrac{1}{2}\lambda_{max}(\boldsymbol{\Gamma}^{-1})\|\boldsymbol{\Theta}\|^2\leqslant\tfrac{1}{2}\max(1,\lambda_{max}(\boldsymbol{\Gamma}^{-1}))(z_1^2+z_2^2+\|\tilde{\boldsymbol{\Theta}}\|^2).$$

Hence, from Eq. (A.6), and using the previous observation

$$\dot{V}\leqslant -c_0V+d_0, \tag{A.7}$$

where

$$\begin{aligned}c_0 &\triangleq 2\frac{\min\big(c_1,c_2,\tfrac{3}{4}\bar{\sigma}\big)}{\max(1,\lambda_{max}(\boldsymbol{\Gamma}^{-1}))},\\ d_0 &\triangleq \tfrac{39}{4}\bar{\sigma}M^2+2\varepsilon_2+4\varepsilon_1.\end{aligned}$$

From Eq. (A.7),

$$V\leqslant V(0)\mathrm{e}^{-c_0t}+\frac{d_0}{c_0}(1-\mathrm{e}^{-c_0t})\leqslant V(0)\mathrm{e}^{-c_0t}+\frac{d_0}{c_0}. \tag{A.8}$$

From the above expression $V(t)$ is shown to be uniformly bounded, which implies that z_1, z_2, $\tilde{\boldsymbol{\Theta}}$ are bounded. Thus, the state variables x_1, x_2, and the parameter estimate $\hat{\boldsymbol{\Theta}}$, are also bounded. As a consequence the boundedness of the control $u(t)$ is obtained which ends the proof. □

Proof of Theorem 2. (a) First it is necessary to claim that $\Delta_2 \triangleq \sigma_\Theta \tilde{\boldsymbol{\Theta}}^{\mathrm{T}} \hat{\boldsymbol{\Theta}} \leqslant 0$. Indeed, if $\|\hat{\boldsymbol{\Theta}}\| \leqslant M$ then $\sigma_\Theta = 0$, and therefore $\Delta_2 = 0$. On the contrary, if $\|\hat{\boldsymbol{\Theta}}\| \geqslant M$ then $\sigma_\Theta > 0$, and

$$\tilde{\boldsymbol{\Theta}}^{\mathrm{T}} \hat{\boldsymbol{\Theta}} = (\boldsymbol{\Theta} - \hat{\boldsymbol{\Theta}})^{\mathrm{T}} \hat{\boldsymbol{\Theta}} = \boldsymbol{\Theta}^{\mathrm{T}} \hat{\boldsymbol{\Theta}} - \|\hat{\boldsymbol{\Theta}}\|^2 \leqslant \|\boldsymbol{\Theta}\| \, \|\hat{\boldsymbol{\Theta}}\| - \|\hat{\boldsymbol{\Theta}}\|^2 = \|\hat{\boldsymbol{\Theta}}\|(\|\boldsymbol{\Theta}\| - \|\hat{\boldsymbol{\Theta}}\|).$$

Observe that from Assumption 2, $\|\boldsymbol{\Theta}\| \leqslant M$. Since the assumption that $\|\hat{\boldsymbol{\Theta}}\| \geqslant M$ is made, $\tilde{\boldsymbol{\Theta}}^{\mathrm{T}} \hat{\boldsymbol{\Theta}} \leqslant 0$ is obtained, and then $\Delta_2 \leqslant 0$, hence the claim is proved.

From Eq. (A.5), and using that $\Delta_2 \leqslant 0$;

$$\dot{V} \leqslant -c_1 z_1^2 - c_2 z_2^2 + 2\varepsilon_2 + 4\varepsilon_1 \leqslant -c_1 z_1^2 + 2\varepsilon_2 + 4\varepsilon_1. \tag{A.9}$$

From the last inequality,

$$z_1^2 \leqslant -\frac{1}{c_1}\dot{V} + \frac{2\varepsilon_2 + 4\varepsilon_1}{c_1}.$$

Integrating at both sides of the above inequality, and dividing by T, gives

$$\frac{1}{T}\int_{t_0}^{t_0+T} z_1^2(t)\,\mathrm{d}t \leqslant -\frac{1}{c_1}\left[\frac{V(t_0+T) - V(t_0)}{T}\right] + \frac{2\varepsilon_2 + 4\varepsilon_1}{c_1}. \tag{A.10}$$

Since (as proved in Theorem 1) V is uniformly bounded, then $\lim_{T\to\infty} V(t_0+T) - V(t_0)/T = 0$, hence taking limits at both sides of Eq. (A.10) we get Eq. (8), which ends the proof of statement (a).

(b) From Eqs. (A.8) and (A.10)

$$\frac{1}{T}\int_0^T z_1^2(t)\,\mathrm{d}t \leqslant -\frac{1}{c_1}\left[\frac{(1-\mathrm{e}^{-c_0 T})V(0)}{T}\right] + \frac{d_0}{c_0 c_1 T} + \frac{2\varepsilon_2 + 4\varepsilon_1}{c_1}.$$

Since $0 \leqslant (1-\mathrm{e}^{-c_0 T})/T \leqslant c_0$,

$$\frac{1}{T}\int_0^T z_1^2(t)\,\mathrm{d}t \leqslant \frac{d_0}{c_0 c_1 T} + \frac{2\varepsilon_2 + 4\varepsilon_1}{c_1}.$$

Using the definition of the constants c_0, d_0, Eq. (9) is reached, which ends the proof of statement (b). □

References

[1] M. Krstic, I. Kanellakopoulos, P. Kokotovic, *Nonlinear and Adaptive Control Design*, Wiley, New York, 1995.

[2] S.S. Ge, C. Wang, Uncertain chaotic system control via adaptive neural design, *International Journal of Bifurcation and Chaos in Applied Sciences and Engineering* 12 (2002) 1097–1109.

[3] F. Ikhouane, M. Krstic, Robustness of the tuning functions adaptive backstepping design for linear systems, *IEEE Transactions on Automatic Control* 43 (1998) 431–437.

[4] P.A. Ioannou, J. Sun, *Robust Adaptive Control*, Prentice-Hall, Englewood Cliffs, NJ, 1996.

[5] H. Khalil, *Nonlinear Systems*, MacMillan, Upper Saddle River, NJ, 1992.

[6] E. Ott, C. Grebogi, J.A. Yorke, Controlling chaos, *Physical Reviews Letters* 64 (1990) 1196–1199.

[7] T. Shinbrot, C. Grebogi, E. Ott, J.A. Yorke, Using small perturbations to control chaos, *Nature* 363 (1993) 411–417.
[8] T.L. Vincent, Control using chaos, *IEEE Control Systems Magazine* 17 (1997) 65–76.
[9] J. Guckenheimer, Ph. Holmes, *Nonlinear Oscillations, Dynamical Systems, and Bifurcations of Vector Fields*, Springer, New York, 1983.
[10] F.C. Moon, P.J. Holmes, A magnetoelastic strange attractor, *Journal of Sound and Vibration* 65 (1979) 285–296.
[11] F.C. Moon, P.J. Holmes, Addendum: a magnetoelastic strange attractor, *Journal of Sound and Vibration* 69 (1980) 339.
[12] M. Battaini, F. Casciati, Chaotic behaviour of hysteretic oscillators, *Journal of Structural Control* 3 (1996) 7–19.
[13] R.W. Wolfe, S.F. Masri, J. Caffrey, Some structural health monitoring approaches for nonlinear hydraulic dampers, *Journal of Structural Control* 9 (2002) 5–18.
[14] X. Tan, J. Zhang, Y. Yang, Synchronizing chaotic systems using backstepping design, *Chaos, Solitons & Fractals* 16 (2003) 37–45.
[15] R.W. Wolfe, Analytical and Experimental Studies of Structural Health Monitoring of Nonlinear Viscous Dampers, Ph.D. Thesis, University of Southern California, 2002.
[16] S.F. Masri, T.K. Caughey, A nonparametric identification technique for nonlinear dynamic problems, *American Society of Mechanical Engineers, Journal of Applied Mechanics* 46 (1979) 433–447.
[17] Y.K. Wen, Method of random vibration of hysteretic systems, *American Society of Civil Engineers, Journal of Engineering Mechanics* 102 (1976) 249–263.
[18] A.H. Barbat, L.M. Bozzo, Seismic analysis of base isolated buildings, *Archives of Computational Methods in Engineering* 4 (1997) 153–192.
[19] A. Isidori, *Nonlinear Control Systems*, 2nd Edition, Springer, Berlin, 1989.
[20] J.M. Kelly, G. Leitmann, A. Soldatos, Robust control of base-isolated structures under earthquake excitation, *Journal of Optimization Theory and Applications* 53 (1997) 159–181.
[21] A.H. Barbat, J. Rodellar, E.P. Ryan, N. Molinares, Active control of nonlinear base-isolated buildings, *American Society of Civil Engineers, Journal of Engineering Mechanics* 121 (1995) 676–684.
[22] N. Luo, J. Rodellar, M. de la Sen, J. Vehí, Output feedback sliding mode control of base isolated structures, *Journal of the Franklin Institute* 337 (2000) 555–577.
[23] F. Benedettini, D. Capecchi, F. Vestroni, Identification of hysteretic oscillators under earthquake loading by nonparametric models, *American Society of Civil Engineers, Journal of Engineering Mechanics* 121 (1995) 606–612.
[24] Y.Q. Ni, J.M. Ko, C.W. Wong, Identification of nonlinear hysteretic oscillators from periodic vibration tests, *Journal of Sound and Vibration* 217 (1998) 737–756.
[25] Y.Q. Ni, J.M. Ko, C.W. Wong, Nonparametric identification of nonlinear hysteretic systems, *American Society of Civil Engineers, Journal of Engineering Mechanics* 125 (1999) 206–215.
[26] J.L. Devore, *Probability and Statistics for Engineering and the Sciences*, Brooks/Cole, New York, 2000.